Shakedown, ratchet, and limit analyses of 90° back-to-back pipe bends under cyclic in-plane opening bending and steady internal pressure

Nak-Kyun Cho and Haofeng Chen*

Department of Mechanical and Aerospace Engineering
University of Strathclyde Glasgow, G1 1XJ, United Kingdom
*Email: haofeng.chen@strath.ac.uk

Abstract

A 90° back-to-back pipe bend structure subjected to cyclic in-plane bending moment and steady internal pressures is analysed by means of the Linear Matching Method (*LMM*) in order to create the limit, shakedown, and ratchet boundaries. The analyses performed in this work demonstrate that the cyclic moment has a more significant impact upon the structural integrity of the pipe bend than the constant pressure. Full cyclic incremental analyses are used to verify the structural responses either side of each boundary and confirm correct responses. In addition, the shakedown boundary produced by the LMM is compared to another shakedown boundary of an identical pipe bend computed by the simplified technique and it is shown that the LMM calculates results more accurately. Parametric studies involving a change of geometry of the pipe bends and loading type are carried out. From the studies of the geometry, two semi-empirical equations are derived from correlations of the reverse plasticity limit and the limit pressure with the bend characteristic. Finally, the results presented in this paper provide a comprehensive understanding of post-yield behaviours of the 90° back-to-back pipe structure under the combined loading as well as offering essential points to be concerned for the life assessment of the piping system.

Keywords: Pipe bend, Shakedown, Ratchetting, Reverse plasticity

1. Introduction

Pipe bends are common components that have been widely used in piping networks, and it is very important to effectively design and assess their load bearing capacity under complex loading conditions. Comparing to straight pipelines, the evaluation of the integrity of pipe bends' tends to be a more complicated process due to the geometrical non-linearity. Moreover, when the pipe bends are subjected to cyclic loads in an elevated temperature, it is likely to cause the yield strain of the material

to be exceeded, leading to severe damage or even failure due to low cycle fatigue or incremental plastic collapse. Hence pipe bends should be designed to avoid structural behaviours such as reverse plasticity or ratchetting, but elastic shakedown is acceptable.

To define the structural response within the post yield behaviours of the material is a complex process and it requires advanced computational analysis such as Incremental Finite Element Analysis (*FEA*). This method allows the structural behaviour under a variety of load combinations to be determined, but requires a lot of computational time especially for complicated models. In additions, it needs a large number of FE simulations to create the structural response boundaries like Bree diagram [1]. Hence, many Direct Methods have been developed and used in order to obtain swift and approximate bounds for the shakedown limit load.

Iterative elastic techniques are a typical approach of Direct Methods and include the Elastic Compensation Method (*ECM*) [2], the Dhalla Reduction Procedure [3], the Gloss R-Node Method [4], and the Linear Matching Method (*LMM*) [5]. The ECM was further modified by Yang et al. as Modified Elastic Compensation Method (*MECM*) [6]. Muscat and Mackenzie presented a superposition method to establish elastic shakedown loads using the lower bound theorem [7]. Muscat et al. introduced a non-linear superposition method [8] based on Polizzotto's research [9] in order to estimate an elastic shakedown boundary of a structure subjected to combined cyclic and steady mechanical load. Abdalla et al. presented shakedown limit loads for two-bar structure problem and the Bree cylinder problem using a simplified technique [10].

These iterative elastic techniques employ elastic perfectly plastic (*EPP*) material models and take into account all possible loading scenarios. Among these methods, the LMM has a distinguished reputation in calculating limit loads and shakedown and ratchet boundaries with high accuracy [11-13]. Owing to its powerful performance, the LMM Abaqus subroutines have been used for an assessment procedure for the high temperature response of structures in R5 [14]. Chen et al. have also proved its performance by presenting accurate limit loads and shakedown boundaries of a single 90° pipe bend [15]. In addition, the LMM has been utilised to analyse cyclic plasticity of various industrial structures including composite materials with or without creep effect [16-19]. Upon these reasons, the LMM is selected to use in this paper to analyse the limit, shakedown, and ratchet boundaries of the 90° back-to-back pipe bends.

Recently, Abdalla et al. presented a shakedown boundary of the 90° back-to-back pipe bends subjected to cyclic in-plane bending moments and steady internal pressures utilising the simplified technique [20]. As claimed by these authors, the 90° back-to-back pipe bends have been widely used in a variety of piping systems of machineries and components on both small and large scales. However, the presented shakedown boundary by the simplified technique remains some points to be improved in terms of accuracy of the data. Moreover, comprehensive structural behaviours of the 90°

back-to-back pipe bends such as the limit and ratchet boundaries have not been published in other research works.

The objective of this paper is to analyse the 90° back-to-back pipe bends subjected to cyclic in-plane opening bending moments and steady internal pressures utilising the proposed method in order to create limit, shakedown and ratchet boundaries with accuracy. The obtained results are verified by full cyclic plasticity analyses using Abaqus step-by-step procedures. Additionally, parametric studies are carried out with varying geometry of the pipe bends and types of loading. Two semi-empirical equations to predict reverse plasticity limit and limit pressures are presented in the parametric studies. Critical points to be concerned for design and life assessment of the pipe bends are discussed.

The novelty of this research work lies in delivering the post yield behaviours of the popular pipe bends with accuracy, the two semi-empirical equations, and the critical reviews in design of the pipe bends from the parametric studies.

2. Numerical Procedures

The calculating procedures of the shakedown and ratchet limit of the LMM have been demonstrated in other papers [21-23]. In this section, the numerical procedures of the LMM being employed in this paper to calculate the upper bound of both shakedown and ratchet limits are briefly overviewed.

2.1. Shakedown Limit Analysis

The LMM is a numerical analysis procedure following theoretical principals that represent nonlinear material responses using a series of linear elastic analyses where the elastic modulus at each integration point is allowed to be iteratively changed. This procedure repeats iteratively, which results in the redistribution of the stress level across a structure with the updated modulus, obtaining accurate upper and lower bounds to the shakedown and ratchet limits.

Let's assume that the structure has a volume of V with a surface area of S. The material of the structure follows the EPP model and satisfies the von-Mises yield condition. The structure is subjected to both thermal loads $\lambda\theta\ (x\ ,t)$ and mechanical loads $\lambda P(x,t)$ which are applied over a time period $0 \le t \le \Delta t$. Both loads are imposed on the volume of V and a part of the surface area of S_T, and remaining surface S_R ($S_R = S - S_T$) is constrained by zero displacement rate ($\dot{u} = 0$). Upon the loads and boundary conditions, a linear elastic solution can be calculated by Eq. (1), where $\lambda\hat{\sigma}_{ij}^{\theta}$ and $\lambda\hat{\sigma}_{ij}^{P}$ are the elastic solutions corresponding to the thermal load and mechanical load respectively.

$$\lambda \hat{\sigma}_{ij}(x,t) = \lambda \hat{\sigma}_{ij}^{\theta}(x,t) + \lambda \hat{\sigma}_{ij}^{P}(x,t) \tag{1}$$

For cyclic loading case, the cyclic stress solution over the time cycle Δt can be expressed by Eq. (2), where $\rho_{ij}^{r}(x,t)$ is the changing residual stress during a cycle and $\overline{\rho}_{ij}(x)$ is the constant residual stress in equilibrium with no surface traction occurring on the S_T corresponding to the residual stress field at the beginning and end of the cycle. In the case of shakedown analysis, $\rho_{ij}^{r}(x,t)$ must be zero through the cycle.

$$\hat{\sigma}_{ij}^{\Delta} = \lambda \hat{\sigma}_{ij}^{\Delta}(x,t) + \overline{\rho}_{ij}(x) + \rho_{ij}^{r}(x,t) \tag{2}$$

Based on Koiter's Theorem [24], the shakedown upper bound multiplier λ_{SD}^{UB} can be obtained by Eq.(3), where $\dot{\varepsilon}_{ij}$ is a kinematically admissible strain rate and $\overline{\dot{\varepsilon}}$ is the effective strain rate $\overline{\dot{\varepsilon}} = \sqrt{\frac{2}{3}\dot{\varepsilon}_{ij}\dot{\varepsilon}_{ij}}$.

$$\lambda_{SD}^{UB} = \frac{\int_{V}\int_{0}^{\Delta t} \sigma_y \overline{\dot{\varepsilon}}(\dot{\varepsilon}_{ij})\, dt dV}{\int_{V}\int_{0}^{\Delta t} (\hat{\sigma}_{ij}^{\Delta}\dot{\varepsilon}_{ij})\, dt dV} \tag{3}$$

This iterative process continues updating the upper bound in a sequence until converging to the least upper bound, satisfying $\lambda_{SD}^{UB} \geq \lambda_{SD}$ where λ_{SD} is the exact shakedown limit. The lower bound multiplier λ_{SD}^{LB} is calculated based on Melan's Theorem [25]. Using the constant residual stress field, the lower bound shakedown limit can be calculated by increasing the lower bound multiplier until the steady state cyclic stresses over the body are no more than the yield stress of the material. Then the lower bound shakedown limit multiplier can be expressed as Eq. (4).

$$f(\lambda_{SD}^{LB}\hat{\sigma}_{ij}^{\Delta}(x\ ,t) + \overline{\rho}_{ij}(x)) \leq 0 \tag{4}$$

2.2. Ratchet Limit Analysis

Unlike the shakedown limit analysis, the ratchet limit analysis considers both the changing residual stress $\rho_{ij}^{r}(x,t)$ and the constant residual stress $\overline{\rho}_{ij}(x)$ which are evaluated separately in a two-step procedure. The first step calculates the varying residual stress and corresponding plastic strain range in a steady cycle for a predefined cyclic load condition. The second step evaluates the ratchet limit caused by an extra constant load, using an extended shakedown procedure, where the cyclic elastic

solution is augmented by the changing residual stress computed in the first step. The stress solution term in Eq. (2) can be written including the enhanced residual stress given by Eq. (5):

$$\hat{\sigma}_{ij}^{\Delta}(x_i,t) = \lambda_{RC}^{UB}\hat{\sigma}_{ij}^{F}(x) + \hat{\sigma}_{ij}^{\Delta}(x,t) + \rho^{r}{}_{ij}(x,t) + \overline{\rho}_{ij}(x) \tag{5}$$

where λ_{RC}^{UB} denotes the upper bound ratchet limit multiplier subjected to the additional constant load $\hat{\sigma}_{ij}^{F}(x)$ and $\hat{\sigma}_{ij}^{\Delta}(x,t)$ is the elastic stress solution corresponding to the cyclic loading condition.

Chen et al.[26, 27] presented the Direct Steady Cycle Analysis (*DSCA*) which can evaluate the varying residual stress utilising the LMM framework. This method adopts a series of iterative cycles defined as n = 1, 2, … , N. Within each iterative sub cycle *n*, *m* number of load instances (m = 1, 2, … , M) are defined. The individual varying residual stress associated with each elastic solution for each load instance is computed iteratively from m =1 to M until the structural response becomes steady state at cycle N. Defining the von-Mises yield condition with the associated flow rule, the upper bound ratchet limit multiplier can be derived by Eq. (6):

$$\lambda_{RC}^{UB} = \frac{\int_V \sum_{m=1}^{M} (\sigma_y \overline{\varepsilon}(\Delta\varepsilon_{ij}^{m}(x,t_m)))\,dV - \int_V \sum_{m=1}^{M} ((\hat{\sigma}_{ij}^{\Delta}(x,t_m) + \rho_{ij}^{r}(x,t_m))\Delta\varepsilon_{ij}^{m}(x,t_m))\,dV}{\int_V \overline{\hat{\sigma}_{ij}^{F}}(x)(\sum_{m=1}^{M}\Delta\varepsilon_{ij}^{m}(x,t_m))\,dV} \tag{6}$$

where $\overline{\varepsilon}(\Delta\varepsilon_{ij}^{m}) = \sqrt{\frac{2}{3}\Delta\varepsilon_{ij}^{m}\Delta\varepsilon_{ij}^{m}}$ and $\Delta\varepsilon_{ij}^{m}$ is the kinematically admissible plastic strain rate history. The upper bound ratchet limit multiplier represents the endurance capacity of the body subjected to the additional constant load without the ratchetting behaviour. On the basis of these formulations, when the structural response becomes steady state, the iteration process begins using Eq. (6) in order to reduce the upper bound multiplier. The process proceeds until converging to the least upper bound ratchet limit. For the lower bound ratchet limit multiplier, the changing residual stress field should be considered together with the constant residual stress. Then the Eq. (4) can be modified to express the lower bound multiplier given by Eq. (7).

$$f(\lambda_{RC}^{LB}\hat{\sigma}_{ij}^{F} + \hat{\sigma}_{ij}^{\Delta}(x,t) + \overline{\rho}_{ij}(x) + \rho_{ij}(x,t)) \le 0 \tag{7}$$

3. Finite Element Model

3.1. Geometry of the 90° back-to-back pipe bends

Fig. 1 shows the 90° back-to-back pipe bends with the two straight pipe ends. Generally pipe bends are expressed in terms of two ratios: *R/r* and *r/t*, where *R* is the bend radius, *r* is the mean radius of the

pipe, and t is the wall thickness. D_m is the mean diameter of the pipe and L_m and L are the length of the horizontal pipe section between the pipe bends and the vertical pipe sections attached to the both pipe bends respectively. With those ratios, the bend characteristic of the pipe is defined as a term of h:

$$h = \frac{R / r}{r / t} = \frac{Rt}{r^2} \tag{8}$$

Due to the symmetry of the geometry about the x-y plane, a half geometry model is considered. A 3D solid model is used to create the model using Abaqus. Key dimensions of the 90° back-to-back pipe bends are summarized in Table 1.

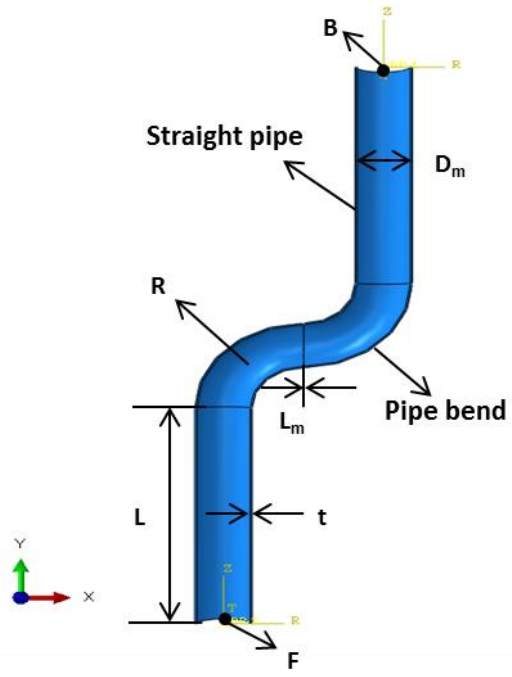

Fig. 1. Half model of the 90° back-to-back pipe bends with two attached vertical straight pipe sections.

Fig. 2 depicts meshed pipe bends with 3D solid element. The pipe structure is meshed with C3D20R quadratic elements for the structure analysis and DC3D20 elements for the heat transfer analysis. Three elements are used to mesh through the thickness. The radius of the pipe bends and the circumferential of the half pipe are meshed with twenty five elements each. The vertical straight pipe sections are meshed with twenty five elements each using the Bias sizing function so that the intersection between the pipe bend and the straight pipe is formed a denser mesh. Through the refinement study the structure is meshed with 7500 elements.

Table 1. Key dimensions of the 90° back-to-back pipe bends and the two straight pipes (all dimensions in mm).

D_m	t	R	L_m	$L = 5D_m$
263.78	9.27	381	0	1318.9

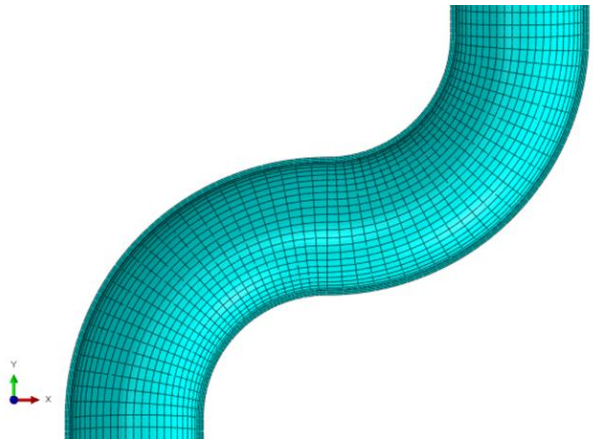

Fig. 2. Enlarged view of the 90° back-to-back pipe bends with 3D solid element mesh.

3.2. Material properties

The key properties of the material are listed in Table 2. The material used in this work is the same material properties of type 304 stainless steel as Abdalla et al. presented in their works excluding the temperature dependent parameters [20]; no thermal effect is applied but the same yield stress σ_y at 20°C is adopted. The material model is assumed to follow the EPP behaviour. The material properties at room temperature are used for the shakedown and ratchet limit analyses including the parametric studies for the geometry change of the pipe bends. The temperature related parameters are applied to a study when the pipe structure is subjected to the loading condition involving a constant thermal loading.

Table 2. Component material properties and temperature dependent yield stresses, where *E* and *v* denote temperature independent Young's modulus and Possion's ratio respectively and thermal conductivity, *k*, and coefficient of thermal expansion, *a*, are values at 100°C.

E [GPa]	v	α [°C^{-1}]	k [Wm^{-1}K^{-1}]
193.74	0.2642	1.73e-05	16.2

Temp [°C]	20	50	100	150	200
Yield Stress [MPa]	271.93	208	199	178	162

3.3. Boundary and loading conditions

A symmetry boundary condition of all nodes located on x-y plane of the 90° back-to-back pipe bend is applied. As shown in Fig. 1, two cylindrical coordinate systems are created at both the top and

bottom of the pipe model. A reference node is created at the origin of each cylindrical coordinate system as B for the top and F for the bottom. All nodes placed on the bottom surface of the pipe structure are constrained by utilising Kinematic Coupling to follow all motions of the node F except the expansion/contraction in the radial direction. The same constraint is applied to all nodes on the top surface, which are restrained against motions of the node B but allowed the pipe to move freely in the radial direction. Verification work for the boundary conditions is performed with a straight pipe and it is confirmed as more or less the same bending stress as a theoretical stress value.

For implementing the cyclic in-plane opening bending moment, a clockwise moment about the z axis on the node B is applied. Fig. 3 illustrates the cyclic bending moment pattern employed for the limit, shakedown, and ratchet analyses. The computed limit moments are normalised by a reference moment which is a formula to calculate a limit moment M_L for the thin wall straight pipe as given by Eq. (9). Due to the half model being employed for the analysis, half moment for the entire structure is taken into account.

$$M_L = \sigma_y D_m^2 t \tag{9}$$

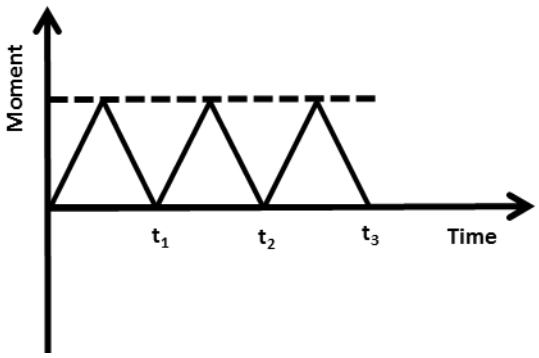

Fig. 3. Cyclic in-plane opening bending moment applied within the limit, shakedown, and ratchet analyses.

The steady internal pressures are applied on the inner surfaces of the pipe with a corresponding axial tension, which is proportional to the internal pressure, on the top surface of the upper straight pipe due to the close-end condition. The internal pressures are normalised with respect to the both reference limit pressure and axial tension for the thin wall straight pipe as given Eqs. (10) and (11). The steady internal pressure and corresponding axial tension will be called as internal pressures P_L from now on.

$$P_I = \frac{2}{\sqrt{3}}(2\sigma_y t / D_m) \tag{10}$$

$$F_A = P_I D_m / 4t \tag{11}$$

The thin wall straight pipe having dimensions of the L, D_m, and t is analysed for different ratios of varying cyclic moment and internal pressures using the LMM and the created limit load boundary are presented in Fig. 4, which satisfies the normalised limit moment and pressures for values of 1.0. One of the parametric studies will carry out the structural analyses for the geometry of r/t = 5 which is not considered as the thin wall pipe, but the Eqs. (9), (10), and (11) will be used for the normalisation due to the fact that the reference loads do not affect the true limit moments and pressures.

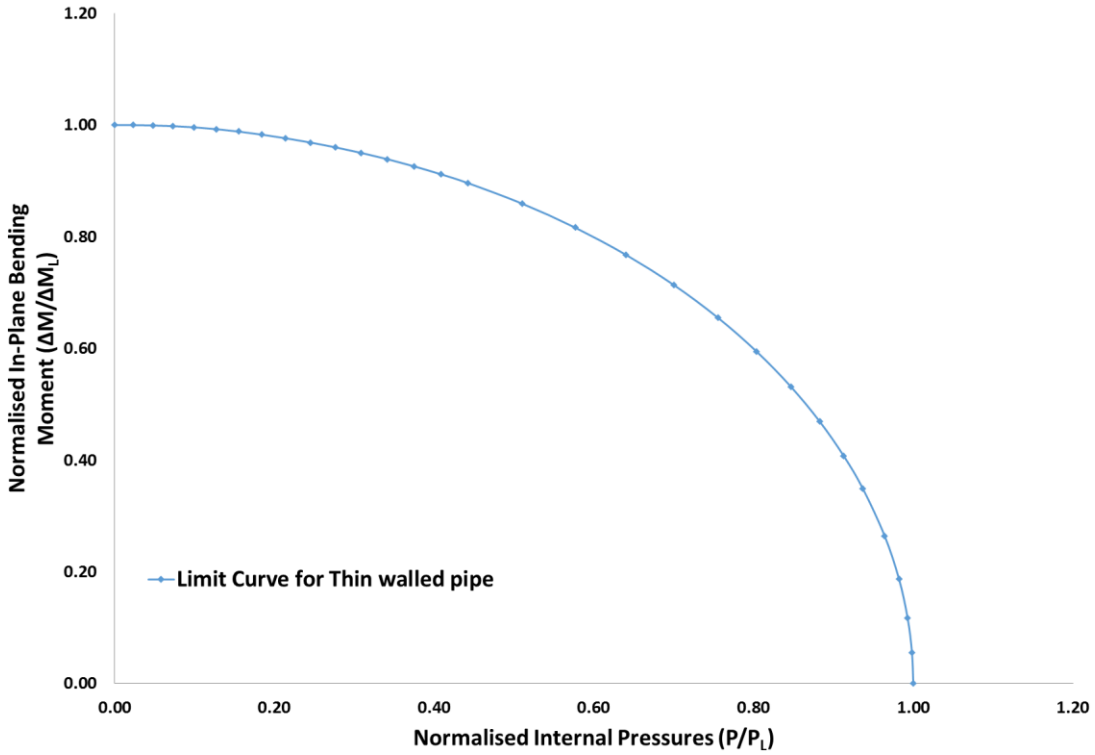

Fig. 4. Limit load interaction curve computed by the LMM for the thin walled straight pipe normalised by the reference loads from Eqs. (9), (10), and (11).

4. Numerical results

4.1. Limit load, shakedown, and ratchet limit interaction curves

Fig. 5 depicts two linear elastic solutions for the 90° back-to-back pipe structure which is subjected to the cyclic bending moments and the steady internal pressures. The bending moments cause the maximum equivalent stress level at the flank of the right side pipe bend due to the clockwise moment. The internal pressures impose the highest stress level at the flank of the left side pipe bend due to the corresponding axial tension creating the anticlockwise moment.

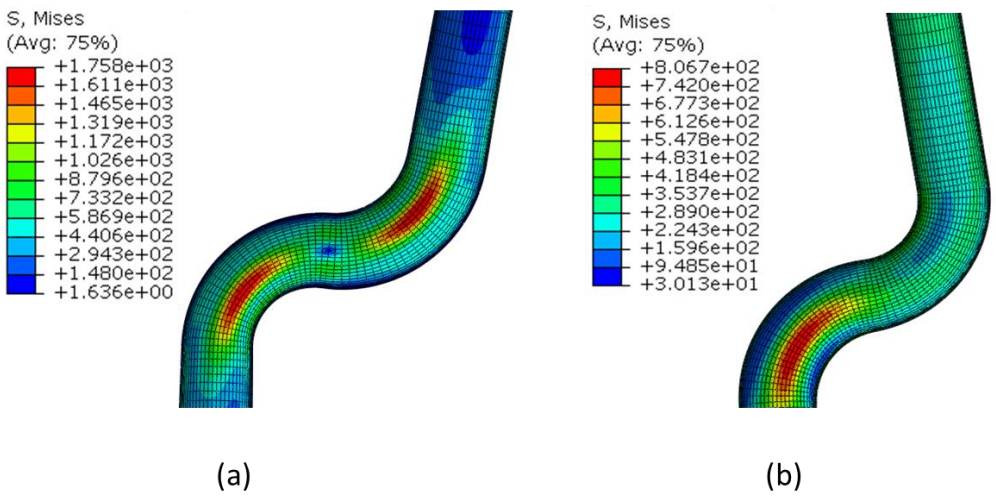

Fig. 5. Equivalent stress [*MPa*] contours from linear elastic stress analyses for a) in-plane opening bending moment M_L b) internal pressures P_L.

Fig. 6 illustrates the limit load, shakedown, and ratchet limit interaction curves for the 90° back-to-back pipe model under the cyclic in-plane opening bending moment and the steady internal pressures produced by the LMM and the shakedown limit curve presented by the simplified technique[20]. Comparing to the normalised limit moment and pressures for the thin walled straight pipe, the endurance capability of the pipe bends decreases to 47% and 76%, respectively. Thus we can see that the cyclic moment can cause severe impacts on structural integrity of the pipe bends. A notable point associated with the limit load curve is that a few normalised moments and pressures are larger than their normalised limit moment and pressures. This can be understood that the clockwise bending moments are compensated by the axial pressure inducing the anticlockwise moment under the combined loading condition.

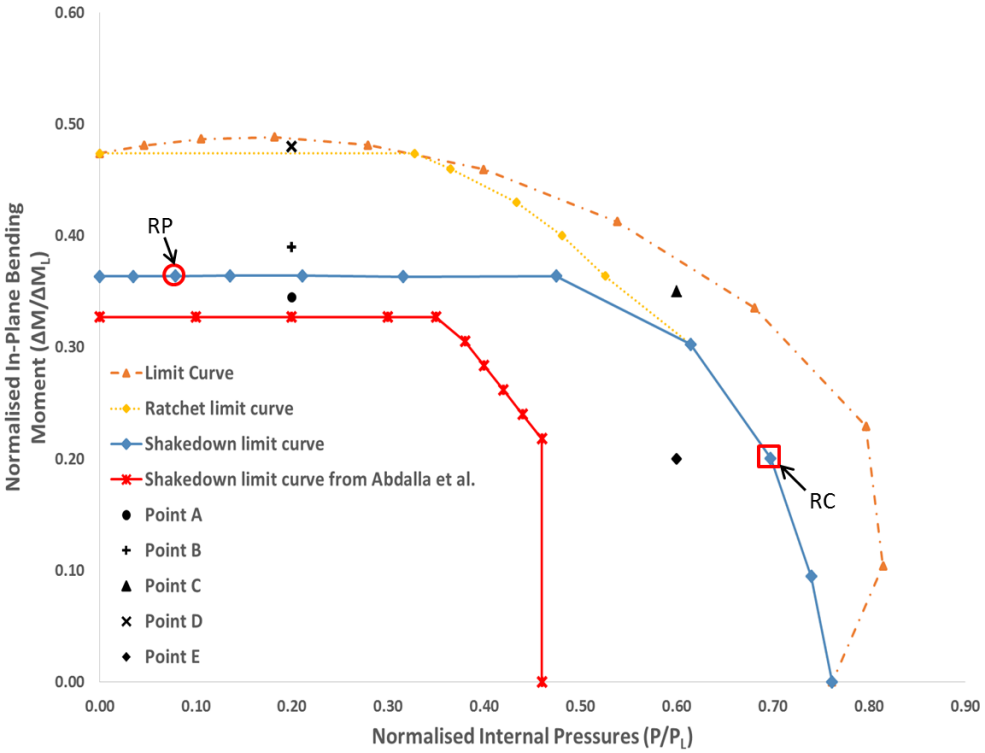

Fig. 6. The limit, shakedown, and ratchet boundaries computed by the LMM and the shakedown boundary presented by Abdalla et al. using the simplified technique for the 90° back-to-back pipe structure under the cyclic in-plane bending moments and steady internal pressures.

The shakedown boundary follows a Bree like diagram where the cyclic moment is a constant value as shown by the horizontal line continuing till the P/P_L = 0.47. The normalized moment of the shakedown boundary at zero pressure is the reverse plasticity limit where plastic strains begin to settle into a closed cycle, also known as "alternating plasticity". The area between the shakedown and ratchet boundaries is called the reversed plasticity zone where it will cause the alternating plasticity mechanism to occur if any combined load is placed within. A contour of plastic strain shown in Fig. 7(a) shows that critical strain accumulation occurs at inner flank of the right side pipe bend where the peak elastic stress appears in Fig. 5(a). The reverse plasticity mechanism is mainly caused by the location of the peak stress due to the bending moment.

The ratchet boundary is different from the typical Bree like shape as the cyclic moment at zero pressures is intersected with the y axis. This is because that the applied cyclic load is not the cyclic thermal load. The ratchet boundary appears similar shape with the shakedown envelope by forming the horizontal line until the P/P_L = 0.33 and the curve converges to the shakedown boundary from the P/P_L = 0.61 to the P/P_L = 0.76. The limit, shakedown, and ratchet boundaries at zero moment are converged to a normalised pressure value which is called the limit pressure where beyond the limit the plastic strains increase till causing plastic collapse. The area beyond the ratchet curve and underneath

the limit load boundary is called the ratchetting zone. A contour of plastic strain shown in Fig. 7(b) shows that critical strain accumulation occurs at inner flank of the left side pipe bend where the peak elastic stress appears in Fig. 5(b). Chen et al. [28] claimed with experimental results that the location of ratchetting strain occurs at intrados of a single 90° pipe bend where strain accumulation starting from outer surface. However, the critical ratchetting mechanism of the 90° back-to-back pipe bends occurs at the inner flank of the left side pipe bend due to the fact that the anticlockwise moment by the corresponding axial tension which has dominant effect rather than internal pressure. Therefore it should be noted that the main ratchetting behaviour can be observed from both intrados and flank of the left side pipe bend under the designed loading condition.

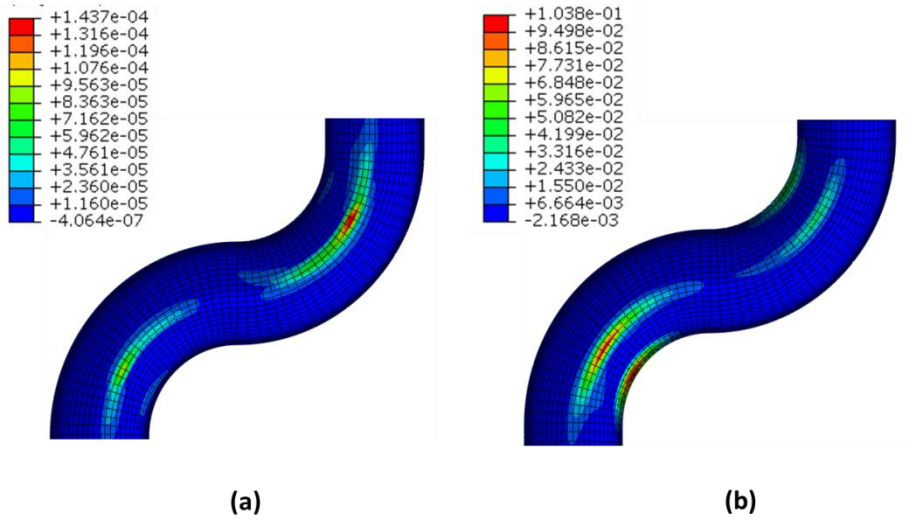

Fig. 7 Plastic strain magnitude (*PEMAG*) contours to show structural responses at: (a) cyclic loading point of RP in Fig. 6 and (b) cyclic loading point of RC in Fig. 6.

4.2. Verification of results and comparative studies

In order to verify the accuracy of the shakedown and ratchet boundaries calculated by the LMM, five points are selected (labelled A, B, C, D, and E in Fig. 6) for the full cyclic plasticity analysis using Abaqus. As claimed by Chen et al.[15], the LMM can calculate the equivalent value to those limit loads with a high accuracy, which shows a difference of less than 1% from the Abaqus Riks analysis. Therefore accuracy of the limit load boundary is not examined within this verification work.

Fig. 8 depicts plastic strain history using Plastic Strain Magnitude (*PEMAG*) in Abaqus for the points A, B, C, D, and E against number of cycles. The PEMAG considers sign of plastic strain in evolution, giving correct total plastic strain accumulation rather than Equivalent Plastic Strain (*PEEQ*). The plastic strain history of the all points is taken from the maximum PEMAG value among the eight Gaussian integration points. The point A and E clearly show the elastic shakedown mechanism and the reverse plasticity mechanism appears in the plastic strain increment plot of point B. The both points C and D display the ratchetting mechanism with the plastic strain rising up within every cycle.

Point D presents a distinguishable increment of the plastic strain thorough the whole number of cycle, whereas the point C appears a small plastic strain increment with every cycle. Due to the small ratchetting zone at the lower pressures and the thin-walled pipe model (r/t=14.2), point C experiences a less significant ratchetting mechanism. However, the plastic strain increment in early cycles exceeds 10% and keeps increasing with the small plastic strain increment. Hence the structural response of point C can be taken into account as the ratchetting mechanism. More clear ratchetting behaviour at the lower pressures is identified from an analysis result obtained for r/t=10 and will be presented in the parametric studies. In addition to the high accuracy, the LMM can produce the results in much less computational time which is less than 10% of the time taken for the same results utilising the full cyclic analyses.

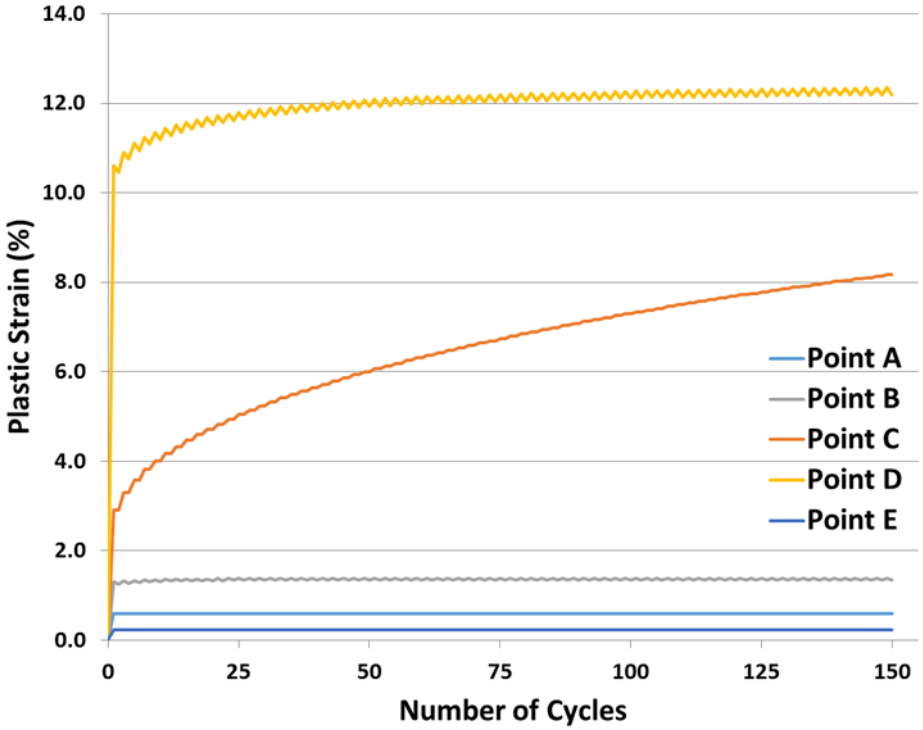

Fig. 8. Plastic strain history (*PEMAG*) of cyclic loading points (A, B, C, D, and E) in Fig. 6 obtained by the full cyclic analysis.

A comparative study between the LMM and the simplified technique[20] is carried out with the shakedown boundary. Due to different lengths of the vertical straight pipe being used for the LMM analysis, the normalized cyclic moment from the Abdalla et al. is increased proportionally to the discrepancy rate of 1.1. As shown by both shakedown limit boundaries in Fig. 6, the simplified technique generated a comparable reverse plasticity limit but is slightly conservative than the LMM as point A shows elastic shakedown behaviour. The conservatism in the reverse plasticity limit from the simplified technique can be understood due to the Abdalla's method have computed the lower bound elastic shakedown but the LMM calculates both upper bound and lower bound shakedown multipliers,

the upper bound shakedown multipliers are used to create the shakedown boundary for Fig. 6. In addition, different element attributes used for the FE model may influence to the result.

For the limit pressure, however, the simplified technique produced 30% smaller normalised limit pressure than one from the LMM out of 100% for the limit pressure of the straight pipe. Verification works for the shakedown boundary with normalised equivalent stress versus PEEQ in Abdala's work do not clearly demonstrate if the stress-strain values are taken from a steady state cycle. Although reverse plasticity or ratchetting response may appear in early cycles, real structural response could be different as going through whole cyclic loading history. Therefore the genuine structural behaviour should be claimed within the steady state cycle.

As shown plastic strain history of point E in Fig. 8, the LMM calculate a structural response of the elastic shakedown for a margin between P/P_L = 0.465 and P/P_L = 0.76. Furthermore what the normalised limit pressures of the limit, shakedown, ratchet boundaries staring from an identical point convince of the LMM providing trustful results. Therefore, the shakedown boundary produced by the LMM can be considered as a less conservative and more reliable structural response than the simplified technique.

5. **Parametric studies and discussions**

Fig. 9 illustrates the varying geometries of the pipe bend structure being used for these parametric studies. For evaluating the effect of *R/r*, the *r/t* is fixed and the effects of varying *R/r* ratio are observed. It carries out the assessment of the effect of the horizontal straight pipe length L_m by changing of the length L_m for the fixed *r/t* ratio. Utilising the same equations from (9) to (11), the reference cyclic moments and steady pressures for each *r/t* ratio are calculated and summarized in Table 3. The obtained moment and pressures by the LMM are normalised by the reference moment and pressures. Due to the half model being employed for these studies, only half of the moment value in Table 3 is considered.

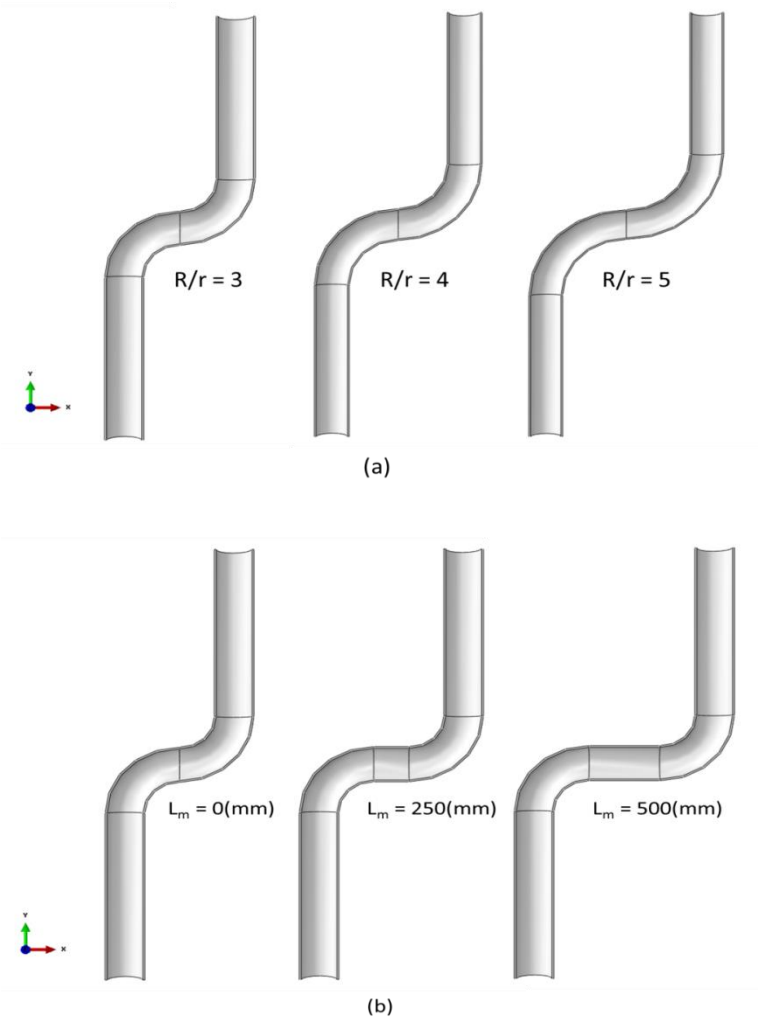

Fig. 9. Geometries of the pipe structure used for the parametric studies; (a) fixed r/t = 10 with varying R/r ratio and (b) fixed r/t = 10 with varying length L_m.

Table 3. Reference loads of cyclic bending moment and steady internal pressure and axial pressure with respect to r/t ratio.

r/t	M_L [Nmm]	P_I [MPa]	F_A[MPa]
5	4.99E+08	62.54	156.36
10	2.50E+08	31.27	156.36
20	1.25E+08	15.64	156.36

5.1. Effects of the geometry of the pipe bends

5.1.1. Effect of R/r and r/t

Fig. 10 shows the limit, shakedown, ratchet boundaries for the fixed *r/t* of 5, 10, and 20 and varying *R/r* of 3, 4, and 5. The other geometries such as the mean diameter of the pipe D_m and the length of the vertical straight pipe *L* are the same as the dimensions in Table 1. As a general trend for each type of geometry, it can be seen that the reverse plasticity limit increases but the limit pressure decreases with a decrease of *r/t* ratio. The larger *R/r* ratio within a fixed *r/t* ratio can withstand a higher cyclic bending moment, but the endurance capacity against the internal pressure become smaller.

For the thick walled pipe (*r/t* = 5), the shakedown boundary at lower pressures ($P/P_L < 0.3$) does not follow the Bree like diagram by not having a constant bending moment. Moreover the shakedown curves converge to the limit curves at the lower pressures. As a result, the ratchet boundary appears very similar to the shakedown boundary. The margins between the limit and shakedown curves become larger after the lower pressures until converging to the limit pressure. Due to the small margin at the lower pressures, the loading condition should be conservatively decided. Another notable point is that the larger *R/r* geometry tends to have constant limit pressures regardless the decrease of cyclic moments from less than $\Delta M/\Delta M_L = 0.75$. Unlike the shakedown boundaries of the single 90° pipe bend structure calculated by the LMM [15], the 90° back-to-back pipe structure has lower limit pressures with an increase of *R/r*. Thus this phenomenon requires consideration when designing the piping systems.

Different from the thick walled pipe, shakedown boundaries for the thin walled pipes (*r/t* = 10 and 20) follow the Bree like diagram by not converging to the limit boundaries at the lower pressures. The margin between the shakedown and limit curves increases with a decrease of *R/r* but with an increase of *r/t*. The ratchet boundaries for the thin walled pipes have a similar shape with the shakedown limit and they are close to the limit boundaries in the region of the lower pressures and then eventually converging to the limit moment at zero pressure. The full cyclic analysis for point F where shown in Fig. 10 (b) is performed to verify the ratchetting behaviour and the result confirms continuous increment of the plastic strain as seen in Fig. 11.

a)

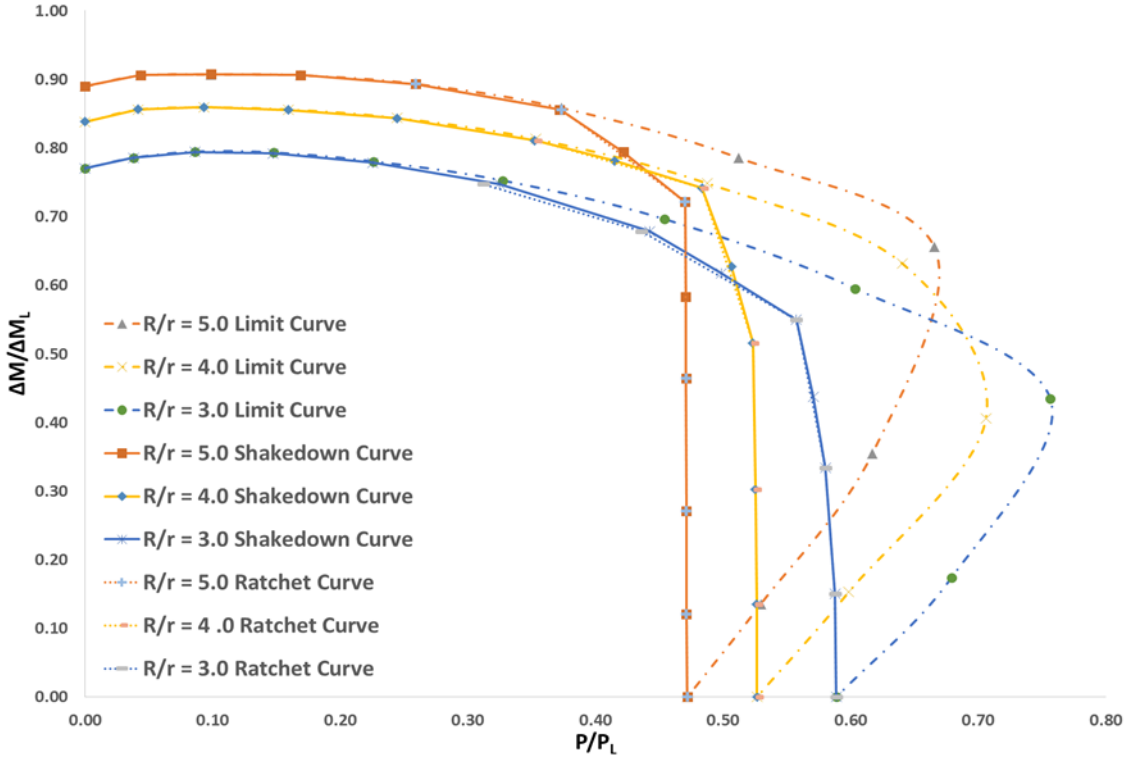
1.00
0.90
0.80
0.70
0.60
0.50
0.40
0.30
0.20
0.10
0.00
ΔM/ΔM_L
0.00
0.10
0.20
0.30
0.40
0.50
0.60
0.70
0.80
P/P_L
R/r = 5.0 Limit Curve
R/r = 4.0 Limit Curve
R/r = 3.0 Limit Curve
R/r = 5.0 Shakedown Curve
R/r = 4.0 Shakedown Curve
R/r = 3.0 Shakedown Curve
R/r = 5.0 Ratchet Curve
R/r = 4 .0 Ratchet Curve
R/r = 3.0 Ratchet Curve

b)

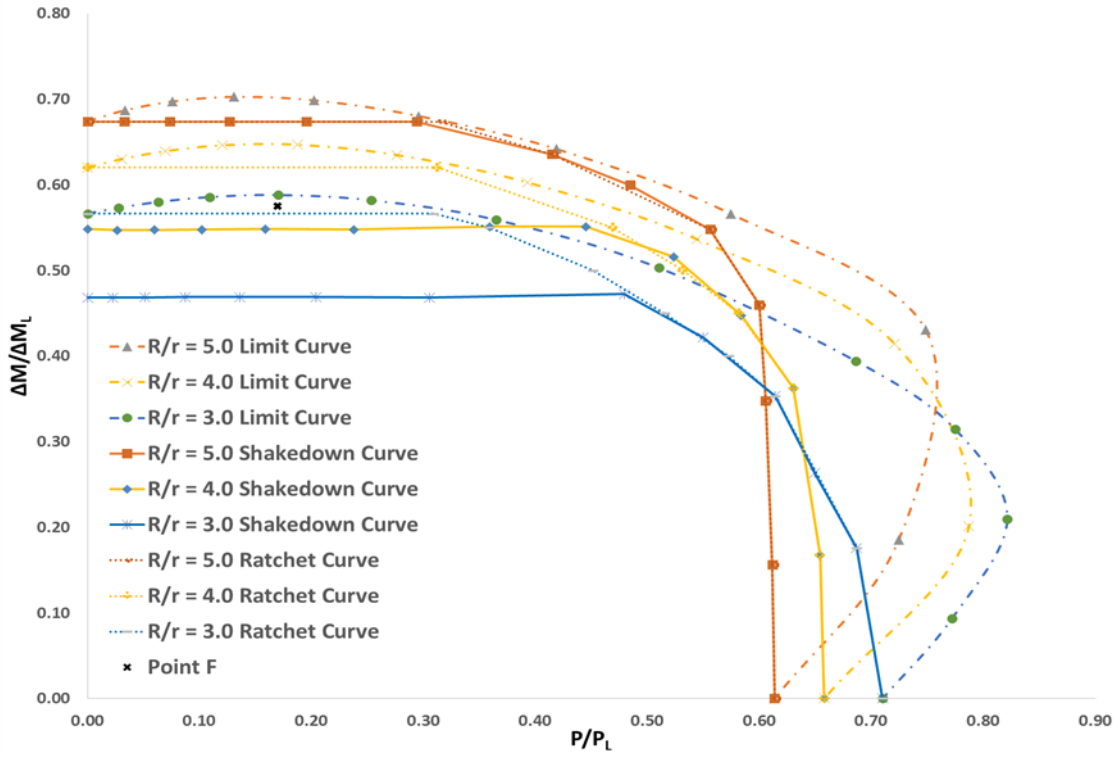
0.80
0.70
0.60
0.50
0.40
0.30
0.20
0.10
0.00
ΔM/ΔM_L
0.00
0.10
0.20
0.30
0.40
0.50
0.60
0.70
0.80
0.90
P/P_L
R/r = 5.0 Limit Curve
R/r = 4.0 Limit Curve
R/r = 3.0 Limit Curve
R/r = 5.0 Shakedown Curve
R/r = 4.0 Shakedown Curve
R/r = 3.0 Shakedown Curve
R/r = 5.0 Ratchet Curve
R/r = 4.0 Ratchet Curve
R/r = 3.0 Ratchet Curve
Point F

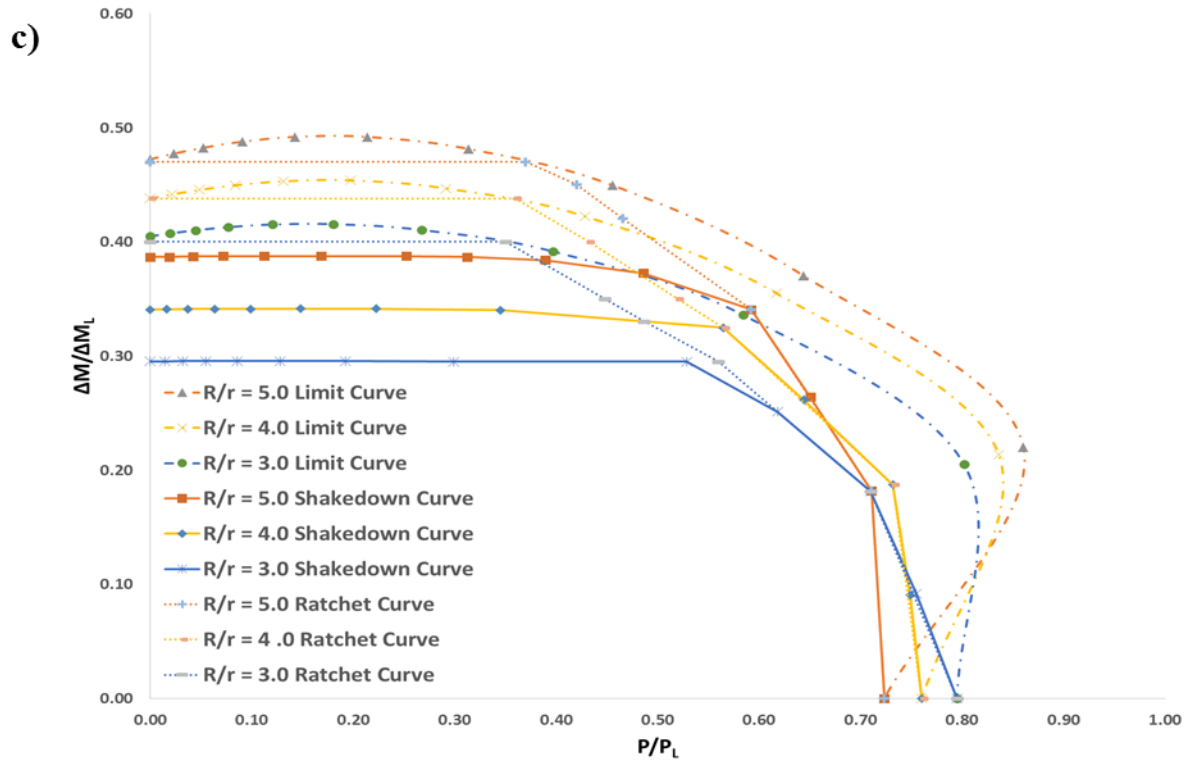

Fig. 10.Effect of varying *R/r* with a) *r/t* = 5, b) *r/t* = 10, and c) *r/t* = 20 under the cyclic bending and steady internal pressures.

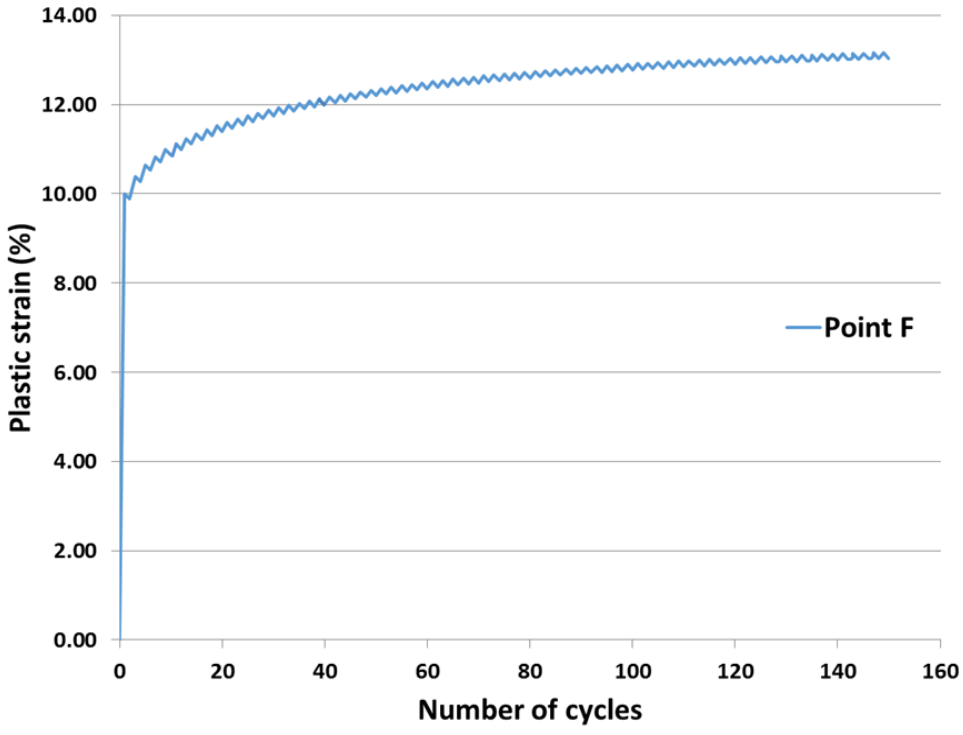

Fig. 11. Plastic strain history (*PEMAG*) of cyclic loading point (E) in Fig. 6 obtained by the full cyclic analysis.

A quadratic relationship between the reverse plasticity limit and the bend characteristic for the single 90° pipe bend structure subjected to cyclic moment and steady internal pressures was derived by Chen et al.[15]. The same approach is made to find correlations among the reverse plasticity limit, limit pressure, and bend characteristic for the 90° back-to-back pipe structure subjected to identical loading conditions. Fig. 12 shows the trends of the reverse plasticity limit and limit pressure against the bend characteristic, and two quadratic polynomial relationships are found, given by Eqs. (11) and (12):

$$RP_{Lim} = -0.784\ h^2 + 1.6242\ h + 0.0492 \tag{11}$$

$$LP_{Lim} = 0.2247\ h^2 - 0.6233\ h + 0.8751 \tag{12}$$

, where RP_{Lim} and LP_{Lim} denote the reverse plasticity limit and limit pressure value respectively. Utilising these derived equations, it would be useful for designers to determine the approximated surface of the shakedown boundary for the back-to-back pipe bend structure having the bend characteristic in the range from 0 to 1 without performing the FE analysis.

From these studies, it is found that the thick walled pipe with a larger *R/r* ratio is suitable for the piping system under the high cyclic moment and lower steady pressures. It is also found that the reverse plasticity limit and the limit pressure have quadratic relationships with the bend characteristic, which can be expressed by two 2nd order polynomial equations.

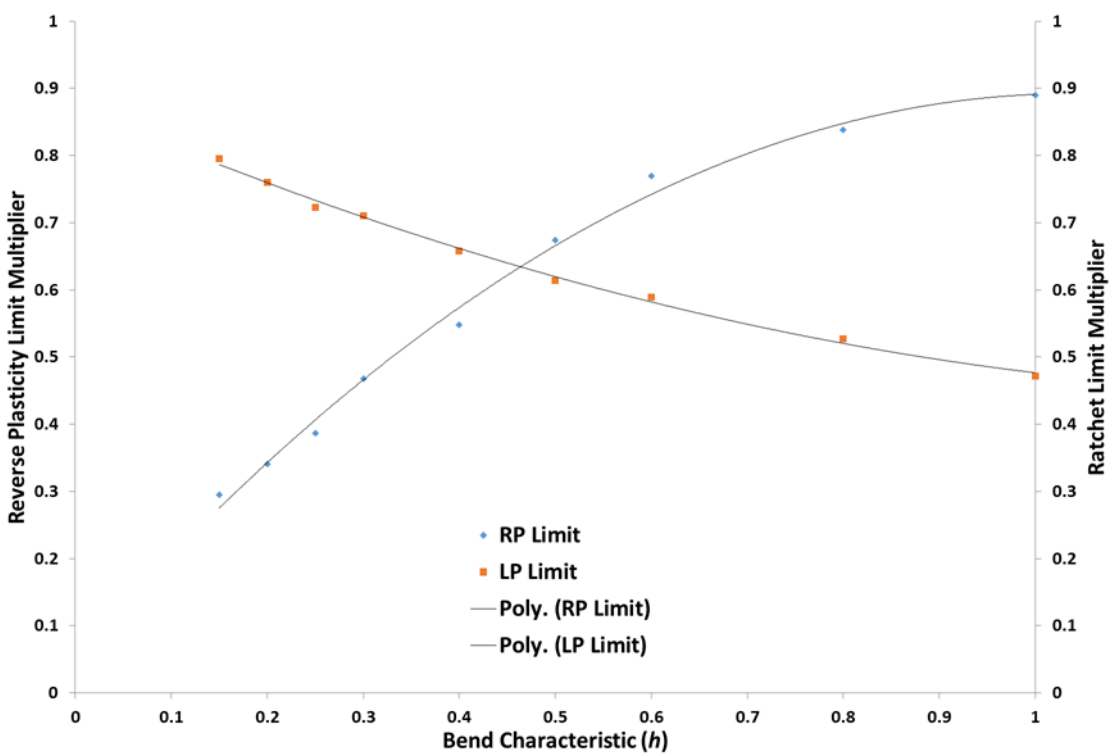

Fig. 12. Reverse plasticity limit and limit pressure trends with respect to bend characteristic in a rage from $h = 0$ to $h = 1$.

5.1.2. Effect of the horizontal straight pipe length L_m

Fig. 13 illustrates the shakedown, ratchet, and limit load boundaries for fixed *r/t* of 5, 10, and 20 and changing horizontal pipe length L_m of 0, 250, and 500[*mm*] for the 90° back-to-back pipe model subjected to the cyclic moment and steady pressure. The other geometries such as the bending radius *R*, mean diameter D_m, and vertical pipe length *L* are identical to the dimensions in Table 1. It is observed as general trends for each type of geometry that the reverse plasticity limit decreases but the limit pressure increases with an increase of *r/t* ratio. The longer pipe length L_m is vulnerable to the steady internal pressures rather than the cyclic moment.

The thick walled pipe (*r/t* = 5) shows more or less the same reverse plasticity limit which is identical to the limit moment regardless of the horizontal pipe length L_m. However the limit pressure decreases with an increase of the length L_m. A very small margin between the shakedown and limit boundaries is also observed at lower pressures (P/P_y < 0.3), thus the ratchet behaviour follows the shakedown behaviour as converging to the limit load boundary. As a result it requires conservative design for selecting the cyclic moment when the pipe structure is subjected to lower pressures.

Both thin walled pipes (*r/t* =10 and 20) show similar trends and shapes of the shakedown, ratchet, and limit load boundaries. The thin walled pipe without the horizontal pipe section provides the larger limit surfaces than the others in all cases. It can be seen that the horizontal pipe sections have effects on the limit pressure but neither on the reverse plasticity limit nor the limit moment. This is because of the left side pipe bend taking significant anticlockwise bending moment due to the axial pressures. As a result the limit pressure decreases with an increase of the length L_m, resulting in that ratchet boundaries tend to become larger as the length L_m decreases for each type of geometry.

These studies provide understandings of the horizontal pipe section between the pipe bends which have significant effects on the limit pressures but minor effects on the cyclic moment. Thus it requires consideration of critical limit pressure levels when designing the pipe bends with the horizontal pipe section.

a)

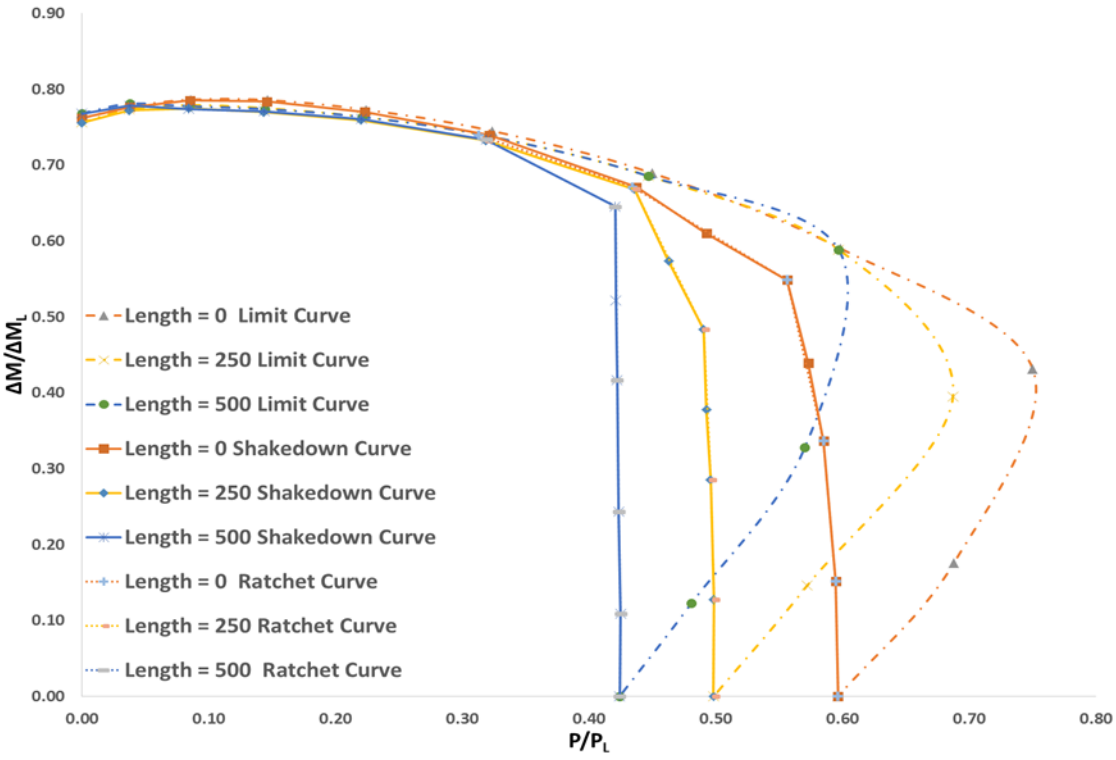
0.90
0.80
0.70
0.60
0.50
0.40
0.30
0.20
0.10
0.00
ΔM/ΔM_L
0.00
0.10
0.20
0.30
0.40
0.50
0.60
0.70
0.80
P/P_L
Length = 0 Limit Curve
Length = 250 Limit Curve
Length = 500 Limit Curve
Length = 0 Shakedown Curve
Length = 250 Shakedown Curve
Length = 500 Shakedown Curve
Length = 0 Ratchet Curve
Length = 250 Ratchet Curve
Length = 500 Ratchet Curve

b)

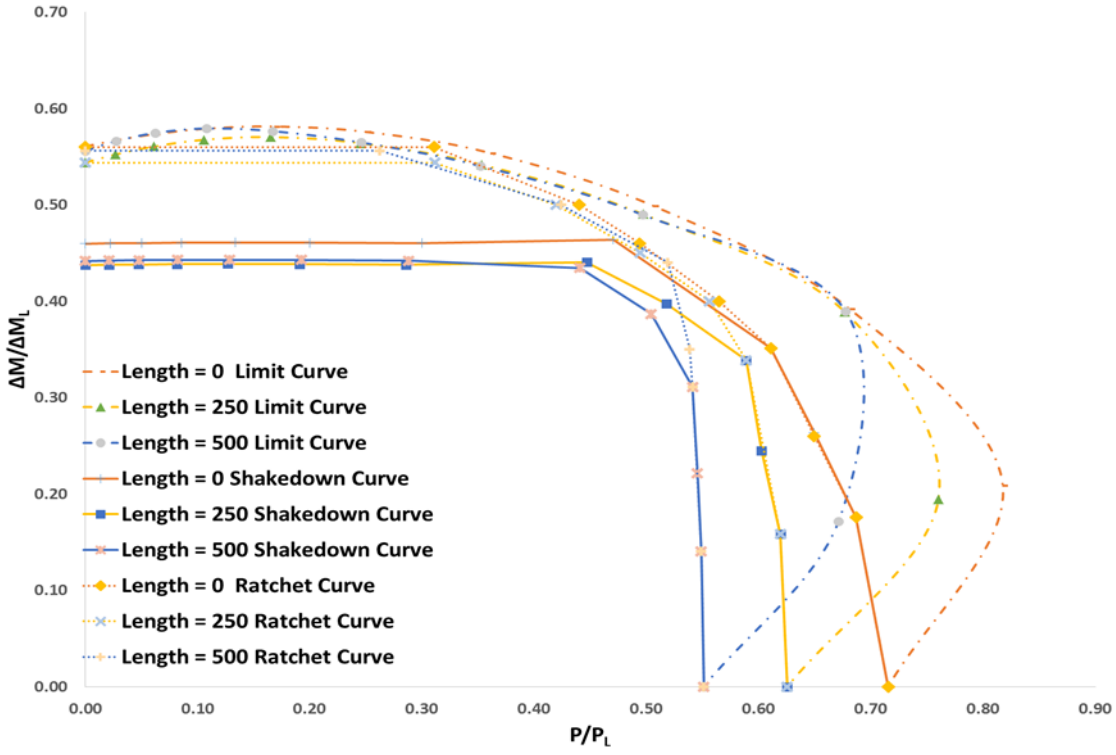
0.70
0.60
0.50
0.40
0.30
0.20
0.10
0.00
ΔM/ΔM_L
0.00
0.10
0.20
0.30
0.40
0.50
0.60
0.70
0.80
0.90
P/P_L
Length = 0 Limit Curve
Length = 250 Limit Curve
Length = 500 Limit Curve
Length = 0 Shakedown Curve
Length = 250 Shakedown Curve
Length = 500 Shakedown Curve
Length = 0 Ratchet Curve
Length = 250 Ratchet Curve
Length = 500 Ratchet Curve

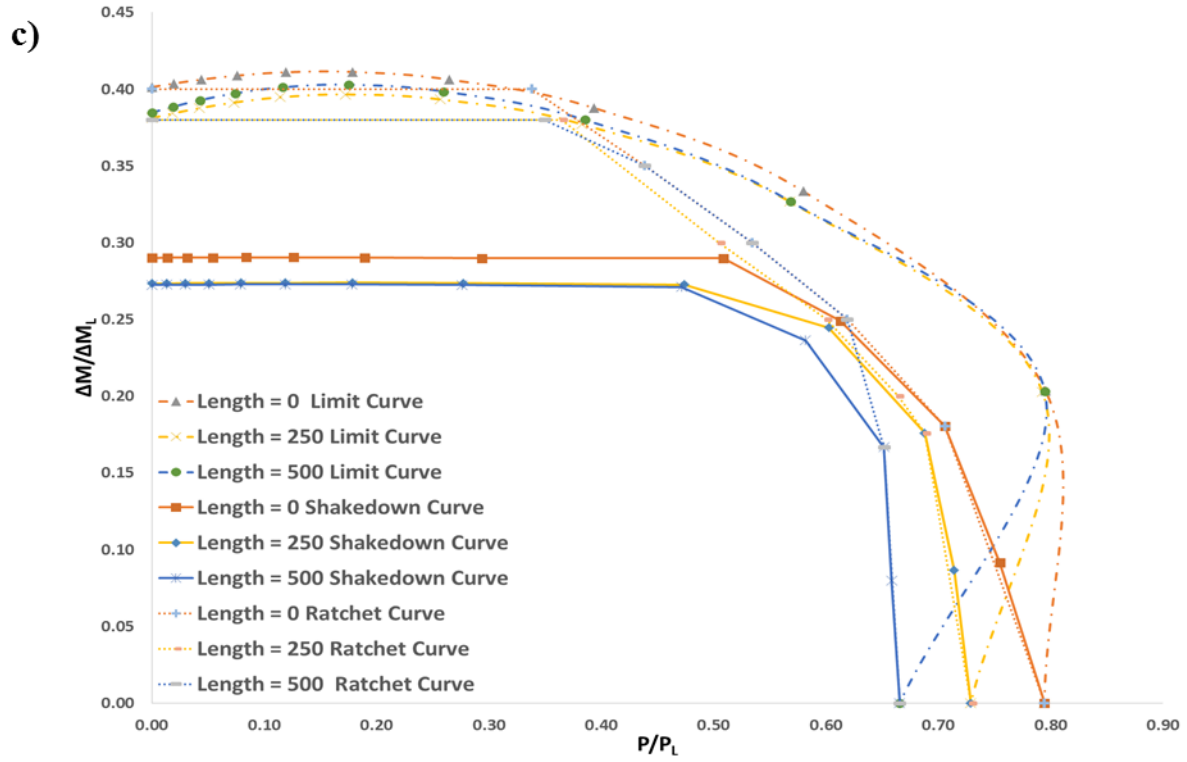

Fig. 13. Effect of varying length Lm with a) *r/t* = 5, b) *r/t* = 10, and c) *r/t* = 20 under the cyclic bending and steady internal pressures.

5.2. Effects of the loading conditions

The parametric study in this section demonstrates the effects of the loading conditions on the limit, shakedown, and ratchet behaviours of the 90° back-to-back pipe bend structure. In practice, the piping system within the power generation facility has running fluid with high temperature such as pressurized boiling water or steam. Taking into account the real operation, the high temperature effect should be applied as an additional thermal loading through the pipe wall. The high temperature in the isothermal condition over the structure may result in a decrease of the yield stress of the material. However, conservatism for the thermal loading is contemplated by implementing the non-isothermal condition which causes the internal stresses across the pipe bends as well as the reduction of the yield stress. The thermal loading is created by implementing a thermal gradient; 100°C and 20°C at the inner and outer surfaces respectively. The other loads such as cyclic moment and steady pressure are the same as before. Temperature dependent yield stresses in Table 2 are utilised for the analyses but the normalisation is done by the Eqs. (9), (10), and (11) with the yield stress at 20°C.

Fig. 14 shows the limit, shakedown, and ratchet boundaries with changing *R/r* and fixed *r/t* =10. It can be seen that the shape of the all boundaries for the each geometry is very similar with Fig. 10(b) where presented the analysed results for the identical geometry without the thermal loading effect. Trend of effects of varying *R/r* under the thermal effect is also similar to before by increasing

endurance capacity against the cyclic moment but reducing the capacity against the steady pressures as *R/r* ratio increases. The main effect of the thermal loading is the overall reduction of the boundaries compared to the ones without thermal effects due to the temperature dependent yield stress. Another notable point is that the reverse plasticity limit of the larger pipe (*R/r* = 5) is not identical to its normalised limit moment. Comparing the shakedown boundaries between with thermal effect and without, the larger *R/r* shows the larger reduction of the reverse plasticity limit but the lower reduction of the limit pressure. Therefore it can be seen that the cyclic moment has critical impacts on the pipe integrity rather than the steady pressure, especially for a pipe with larger *R/r* when applying the temperature dependent yield stress.

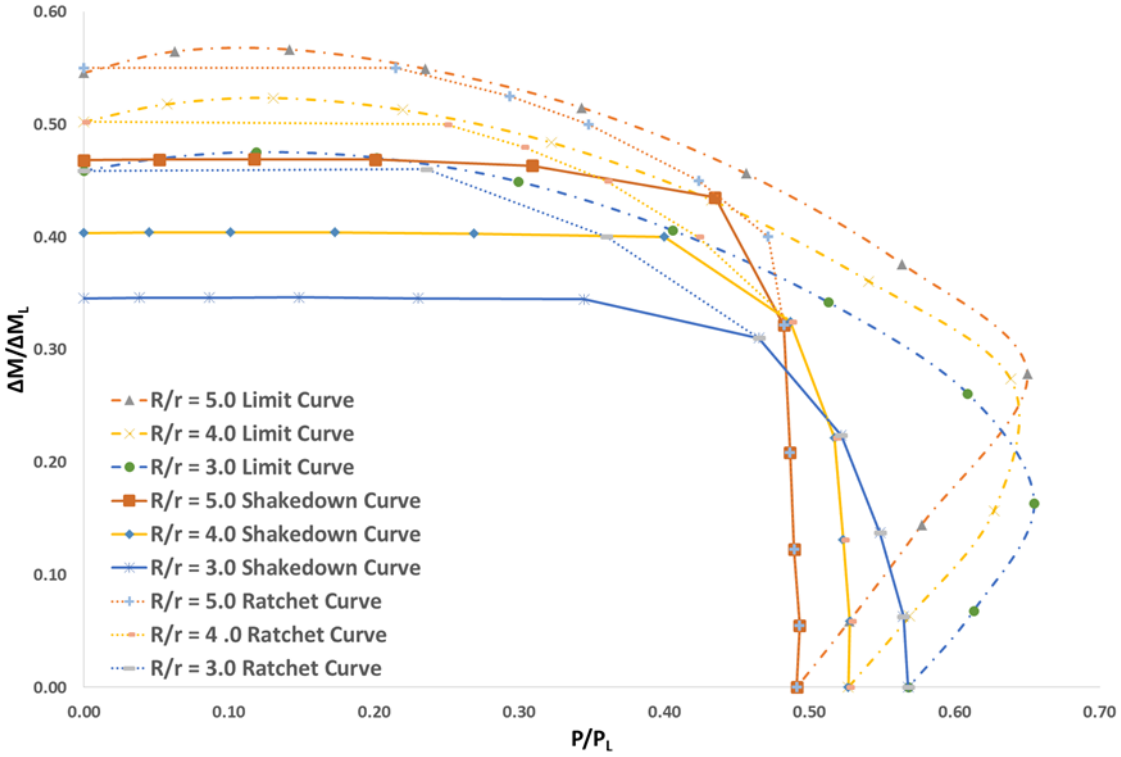

Fig. 14. Effect of varying *R/r* with fixed *r/t* = 10 under the cyclic bending and steady internal pressures involving constant thermal loading.

6. **Conclusions**

The limit, shakedown, and ratchet boundaries are analysed using the LMM for the 90° degree back-to-back pipe bend structure. The results obtained provide the endurance capacity of the pipe model against cyclic moment and internal pressures with respect to the varying geometry and loading types. The results presented in this paper may offer useful information regarding the design and life assessment of the piping systems within designated operating loading conditions, particularly that the derived semi-empirical equations allow to calculate the reverse plasticity limit and limit pressure with

varying *R/r*, *r/t*, and *h*, without performing the finite element analyses. Based on the analysed data, following key remarks are made:

- The Linear Matching Method has been verified by the comparison study and the full cycle incremental analysis, providing the accurate structural response with the limit, shakedown, and ratchet boundaries.
- As *r/t* increase, structural integrity of the pipe model is vulnerable to the cyclic moment rather than the steady pressure. Decreasing *r/t* decreases the margin between the shakedown and limit boundary, especially almost no margin at lower pressures. As a result, the ratchet behaviour tends to follow the shakedown behaviour. Therefore, it requires conservative approach in design of the cyclic loading condition in order to avoid unexpected plastic collapse.
- Increasing *R/r* increases the endurance capacity against the cyclic moment but decreases the capacity against the steady pressures. Moreover, increasing *R/r* decreases the margin between the shakedown and limit envelops, thus the ratchet behaviour forms similar envelop with the shakedown behaviour. Therefore, it requires additional cares to be taken to ensure sufficient margin is secured.
- Normalised moment and pressures corresponding to the reverse plasticity limit and limit pressure respectively have a relationship with the bend characteristic as shown Eqs. (12) and (13).
- Increasing L_m (the horizontal straight pipe section between the pipe bends) has more negative impacts on the endurance capacity against the pressures than the moment. As the wall thickness increase (decreasing *r/t*), the capacity against the pressures become smaller but against the moment is a more or less same regardless the length L_m.
- The additional thermal loading can result in a significant reduction of the limit, shakedown, and ratchet boundaries. Reduction of the normalised moment is larger than the normalised pressures. As *R/r* increases, a reduction rate of the normalised moment becomes larger while normalised pressure is smaller.

Acknowledgement

The authors gratefully acknowledge the support of the University of Strathclyde during the course of this work.

References

1. Bree, J., *Elastic-plastic behaviour of thin tubes subjected to internal pressure and intermittent high-heat fluxes with application to fast-nuclear-reactor fuel elements.* The Journal of Strain Analysis for Engineering Design, 1967. **2**(3): p. 226-238.
2. Mackenzie, D., J. Boyle, and R. Hamilton, *The elastic compensation method for limit and shakedown analysis: a review.* The Journal of Strain Analysis for Engineering Design, 2000. **35**(3): p. 171-188.
3. Dhalla, A. *A simplified procedure to classify stresses for elevated temperature service*. in *ASME transactions, PVP division conference*. 1987.
4. Seshadri, R., *Inelastic evaluation of mechanical and structural components using the generalized local stress strain method of analysis.* Nuclear Engineering and Design, 1995. **153**(2-3): p. 287-303.
5. Chen, H. and A.R. Ponter, *Shakedown and limit analyses for 3-D structures using the linear matching method.* International Journal of Pressure Vessels and Piping, 2001. **78**(6): p. 443-451.
6. Yang, P., et al., *Limit analysis based on a modified elastic compensation method for nozzle-to-cylinder junctions.* International Journal of Pressure Vessels and Piping, 2005. **82**(10): p. 770-776.
7. Muscat, M. and D. Mackenzie, *Elastic-shakedown analysis of axisymmetric nozzles.* Journal of pressure vessel technology, 2003. **125**(4): p. 365-370.
8. Muscat, M., R. Hamilton, and J. Boyle, *Shakedown analysis for complex loading using superposition.* The Journal of Strain Analysis for Engineering Design, 2002. **37**(5): p. 399-412.
9. Polizzotto, C., *On the Conditions to Prevent Plastic Shakedown of Structures: Part I—Theory.* Journal of applied mechanics, 1993. **60**(1): p. 15-19.
10. Abdalla, H.F., M.M. Megahed, and M.Y. Younan, *A simplified technique for shakedown limit load determination.* Nuclear Engineering and Design, 2007. **237**(12): p. 1231-1240.
11. Chen, H., J. Ure, and D. Tipping, *Calculation of a lower bound ratchet limit part 1–Theory, numerical implementation and verification.* European Journal of Mechanics-A/Solids, 2013. **37**: p. 361-368.
12. Ure, J., H. Chen, and D. Tipping, *Calculation of a lower bound ratchet limit part 2–Application to a pipe intersection with dissimilar material join.* European Journal of Mechanics-A/Solids, 2013. **37**: p. 369-378.
13. Ure, J., H. Chen, and D. Tipping, *Verification of the linear matching method for limit and shakedown analysis by comparison with experiments.* Journal of Pressure Vessel Technology, 2015. **137**(3): p. 031003.
14. Ainsworth, R.A. and R5_Panel, *Assessment procedure for the high temperature response of structures*, in *EDF Energy Nuclear Generation Ltd*. 2014.
15. Chen, H., et al., *Shakedown and limit analysis of 90 pipe bends under internal pressure, cyclic in-plane bending and cyclic thermal loading.* International Journal of Pressure Vessels and Piping, 2011. **88**(5): p. 213-222.
16. Barbera, D. and H. Chen, *Creep rupture assessment by a robust creep data interpolation using the Linear Matching Method.* European Journal of Mechanics-A/Solids, 2015. **54**: p. 267-279.
17. Giugliano, D., D. Barbera, and H. Chen, *Effect of fiber cross section geometry on cyclic plastic behavior of continuous fiber reinforced aluminum matrix composites.* European Journal of Mechanics-A/Solids, 2017. **61**: p. 35-46.
18. Giugliano, D. and H. Chen, *Micromechanical modeling on cyclic plastic behavior of unidirectional fiber reinforced aluminum matrix composites.* European Journal of Mechanics-A/Solids, 2016. **59**: p. 155-164.
19. Zhu, X., et al., *Cyclic plasticity behaviors of steam turbine rotor subjected to cyclic thermal and mechanical loads.* European Journal of Mechanics-A/Solids, 2017. **66**: p. 243-255.

20. Abdalla, H.F., *Shakedown boundary determination of a 90° back-to-back pipe bend subjected to steady internal pressures and cyclic in-plane bending moments.* International Journal of Pressure Vessels and Piping, 2014. **116**: p. 1-9.
21. Ure, J., et al., *A direct method for the evaluation of lower and upper bound ratchet limits.* Procedia Engineering, 2011. **10**: p. 356-361.
22. Chen, H., *Lower and upper bound shakedown analysis of structures with temperature-dependent yield stress.* Journal of Pressure Vessel Technology, 2010. **132**(1): p. 011202.
23. Chen, H. and A. Ponter, *The 3-D shakedown and limit analysis using the linear matching method.* Int. J. Pressure Vessels Piping, 2002. **78**: p. 443-451.
24. Koiter, W.T., *General theorems for elastic-plastic solids*. 1960: North-Holland Amsterdam.
25. Melan, E., *Theorie statisch unbestimmter Systeme aus ideal-plastischem Baustoff*. 1936: Hölder-Pichler-Tempsky in Komm.
26. Chen, H., et al., *On shakedown, ratchet and limit analyses of defective pipeline.* Journal of Pressure Vessel Technology, 2012. **134**(1): p. 011202.
27. Chen, H. and A.R. Ponter, *A direct method on the evaluation of ratchet limit.* Journal of Pressure Vessel Technology, 2010. **132**(4): p. 041202.
28. Chen, X., B. Gao, and G. Chen, *Ratcheting study of pressurized elbows subjected to reversed in-plane bending.* Journal of Pressure Vessel Technology, 2006. **128**(4): p. 525-532.